

Thermodynamics and phase transition of topological dilatonic Lifshitz-like black holes

S. H. Hendi^{1,2,3 *}, F. Azari^{1,2}, E. Rahimi^{1,2,4}, M. Elahi^{1,2}, Z. Owjifard^{1,2} and Z. Armanfard⁵

¹*Department of Physics, College of Sciences, Shiraz University, Shiraz 71454, Iran*

²*Biruni Observatory, College of Sciences, Shiraz University, Shiraz 71454, Iran*

³*Canadian Quantum Research Center 204-3002 32 Ave Vernon, BC V1T 2L7 Canada*

⁴*Department of Elementary Particles, Faculty of Physics, University of Kashan, Kashan, Iran*

⁵*Department of physics and astronomy, Washington State University, Pullman, Washington 99164-2814, USA*

It is known that scalar-tensor gravity models can be studied in Einstein and Jordan frames. In this paper, we consider a model of scalar-tensor gravity in Einstein's frame to calculate the Lifshitz-like black hole solutions with different horizon topologies. We study thermodynamic properties and first order van der Waals like phase transition, and find that the Lifshitz parameter affects the phase structure. In addition, we investigate thermal stability by using the behavior of heat capacity and various methods of geometrical thermodynamics.

I. INTRODUCTION

Regarding the successful consequences of the general relativity, especially the gravitational waves [1] prediction, it may be believed that it is a fundamental theory of gravitation. Nonetheless, it has recently been found that GR is neither a renormalizable theory in small-scale (UV regime) nor can explain the late time acceleration of the universe in the large-scale (IR regime). Nowadays, it is a conviction that GR needs a UV-complete gravitational theory and an IR one as well.

Taking into account a Lagrangian with a supplementary higher order derivatives of the metric, one may solve the problem of renormalizability in UV scale. Although some higher derivative modifications of GR provide the renormalizability, their applications may lead to ghosts. This is due to the fact that although the higher spatial derivatives can improve renormalizability, the higher time derivatives will lead to ghosts. Accordingly, one should look for a Lorentz violation theory in such a way that the higher spatial derivatives will be decomposed from higher time ones. In this regard, the Horava-Lifshitz [2, 3] approach helps us to build a theory with an anisotropic scaling between time and space

$$t \rightarrow \lambda^z t, \quad \mathbf{x} \rightarrow \lambda \mathbf{x}, \quad (1)$$

where z is the dynamical critical exponent. Considering Eq. (1), one finds that although the Galilean invariance is preserved, isotropy and Lorentz symmetry between space and time will be broken. It is also notable that $z \geq n$ (n denotes the spatial dimension of the spacetime) is a requirement for the power-counting renormalizability, while the Lorentz invariance can be recovered for $z = 1$ [2–8].

With this in mind, we examine the effect of the critical exponent (z) on the thermodynamics of black holes, a theme that has received considerable attention in recent decades. More specifically, we focus on the possible phase transition of topological Lifshitz-like black holes. Among different classic and quantum aspects of black holes, investigation of thermodynamic properties has always played a central role in the black hole physics. As a window to quantum gravity, the role of black hole thermodynamics, phase transition and criticality cannot be denied. Thermodynamic description of black holes refers to the primitive works of Bekenstein and Hawking on the entropy and temperature of the event horizon [9–11]. Strictly speaking, they showed that the area of event horizon and its surface gravity are, respectively, associated with the entropy and temperature of the black hole. Regarding the total energy (mass) of the black hole as a conserved charge associated with the time-translation symmetry, we can examine the first law of thermodynamics, just as the analogy with the common first law of thermodynamics in usual systems. In a realistic scenario, we should check the robustness of black hole with respect to small perturbation. In other words, we have to study both dynamic and thermodynamic stabilities of the solutions. Dynamical stability can be investigated through the quasi-normal modes of the solutions, while thermodynamic stability may be studied based on the response of a system to the fluctuations of energy, temperature and other thermodynamic parameters near the equilibrium. Based on perturbative variables, thermodynamic stability of a black hole can be studied via micro-canonical, canonical and grand canonical ensembles. In recent years, black hole thermodynamics and the criteria of thermal stability have

* email address: hendi@shirazu.ac.ir

been investigated in literature [12–17]. Regarding a typical black hole as a thermodynamic system, one may look for thermodynamic variables as the first step. In addition to the first law of thermodynamics, the Smarr relation with scaling approach can be helpful in this regard. Based on the Smarr relation of black holes, one has to modify the first law of thermodynamics in the so-called extended phase space. Working in the extended phase space, the cosmological constant interpreted as a dynamical pressure, and AdS charged black holes undergo a van der Waals like phase transition.

Geometrical thermodynamics (GT) is one of the interesting methods to investigate the black hole phase transition. This approach was employed by the works of Gibbs [18] and Caratheodory [19]. Based on this method one could hire thermodynamical potentials and their corresponding quantities to define a phase space. Constructing the thermodynamical metric, the divergence points of its Ricci scalar provide important information related to the possible phase transition of black hole system. The most common thermodynamical metrics are Weinhold, Ruppeiner, Quevedo and HPEM. The first one which is introduced by Weinhold [20, 21] is defined on the space of equilibrium state of thermodynamic systems. After that Ruppeiner defined another metric in 1979 [22, 23]. The shortcomings of both Weinhold and Ruppeiner metrics come from the fact that they are not invariant under Legendre transformation. Since Legendre invariance plays a major role in GT method, Quevedo proposed the first Legendre invariance metric [24, 25] which solved some problems of previous methods. However, Quevedo metric is not, completely, a successful model in several specific systems and its Ricci scalar has extra divergence point without physical interpretation. Finally, a new metric was proposed [26–28] in which the problem of mismatched divergency is not observed [29–31].

This paper is organized as follow. At first, the field equations and the static solutions of the Lifshitz model are presented. Then, the thermodynamic and conserved quantities are calculated, and thermal stability and the existence of phase transition are examined by studying the behaviour of the system through $C_Q - r_+$, $P - V$, $G - T$ diagrams. Finally, the geometrical thermodynamic method is used to confirm the results. We end the paper with some concluding remarks.

II. EXACT SOLUTIONS WITH THEIR GEOMETRIC AND THERMODYNAMIC PROPERTIES

Here, we consider a model of scalar-tensor gravity in which the scalar field is non-minimally coupled with the Maxwell field as [32–35]

$$I = \int_{\mathcal{M}} d^4x \sqrt{-g} \left[R - 2\Lambda - \frac{1}{2} \partial_\mu \phi \partial^\mu \phi + V(\phi) - e^{\lambda\phi} F^{\mu\nu} F_{\mu\nu} \right], \quad (2)$$

where

$$V(\phi) = V_0 e^{\gamma\phi}, \quad (3)$$

and Λ , λ , γ and V_0 are some constant parameters of the theory. The field equations of the above action can be obtained via the variational principle, as

$$R_{\mu\nu} + \frac{1}{2} [V(\phi) - 2\Lambda] g_{\mu\nu} = \frac{1}{2} \partial_\mu \phi \partial_\nu \phi + 2e^{\lambda\phi} \left(F_{\mu\sigma} F_\nu^\sigma - \frac{g_{\mu\nu}}{4} F_{\alpha\beta} F^{\alpha\beta} \right), \quad (4)$$

$$\nabla^2 \phi = -\frac{dV(\phi)}{d\phi} + \lambda e^{\lambda\phi} F_{\alpha\beta} F^{\alpha\beta}, \quad (5)$$

$$\nabla_\mu (e^{\lambda\phi} F^{\mu\nu}) = 0. \quad (6)$$

Now, we consider the following ansatz for the metric,

$$ds^2 = -\left(\frac{r}{r_0}\right)^z B(r) dt^2 + \frac{1}{B(r)} dr^2 + r^2 d\Omega_k^2, \quad (7)$$

where the line element $d\Omega_k^2$ is the metric of two-dimensional (unit) hypersurface with constant curvature $6k$ and volume V_k with the following explicit form

$$d\Omega_k^2 = \begin{cases} dx_1^2 + \sin^2 x_1 dx_2^2, & k = 1 \\ dx_1^2 + \sinh^2 x_1 dx_2^2, & k = -1 \\ dx_1^2 + dx_2^2, & k = 0 \end{cases}, \quad (8)$$

in which different values of the topological factor ($k = -1, 0, +1$) indicate the surface (event horizon) topology as positive (spherical, \mathbb{S}^2), zero (planar, \mathbb{R}^2), or negative (hyperbolic, \mathbb{H}^2). In order to solve the field equations, we

assume that $\phi = \phi(r)$ and the only nonzero components of the gauge field are $F_{rt} = -F_{tr} \neq 0$. As the first step, we consider the Maxwell equation (6) with the subtraction of the tt and rr components of the Einstein equation ($R_{tt} - R_{rr}$) to obtain

$$e^\phi = \left(\frac{r}{r_0}\right)^{\sqrt{2z}}, \quad (9)$$

$$F_{tr} = \frac{q}{r^2} \left(\frac{r_0}{r}\right)^{\lambda\sqrt{2z} - \frac{z}{2}}. \quad (10)$$

Now, we can obtain the metric function $B(r)$ by utilizing the other components of the Einstein equations (4), as

$$B(r) = \frac{2k}{z+2} - \frac{m}{r^{1+\frac{z}{2}}} + \frac{V_0 r^2}{\Gamma} \left(\frac{r}{r_0}\right)^{\gamma\sqrt{2z}} + \frac{2q^2}{\Xi r^2} \left(\frac{r_0}{r}\right)^{\lambda\sqrt{2z}} - \frac{2\Lambda r^2}{6+z}. \quad (11)$$

In these relations, $z > 0$ is the dimensionless Lifshitz parameter, r_0 is an arbitrary constant with length dimension, $\Gamma = 2\gamma\sqrt{2z} + 6 + z$, $\Xi = 2\lambda\sqrt{2z} + 2 - z$, m is an integration constant related to the mass and q is the electric charge of the electromagnetic field (Hint: comparing the mass term with the mass term of 4-dimensional Schwarzschild-like black holes ($\frac{-m_0}{r}$), one finds $m = m_0 r_0^{z/2}$ as a relation between the integration constant, m , and the geometrical mass, m_0).

In order to find the behavior of the curvature, we should calculate the curvature scalars. Calculating the Ricci scalar and Riemann invariant (Kretschmann scalar), we obtain

$$R = -B''(r) - \frac{(3z+8)}{2r} B'(r) - \frac{(z^2+2z+4)}{2r^2} B(r) + \frac{2k}{r^2}, \quad (12)$$

$$\begin{aligned} R_{\alpha\beta\gamma\delta} R^{\alpha\beta\gamma\delta} &= B'^2(r) + \frac{z(z-2)}{r^2} \left(B(r) + \frac{3rB'(r)}{z-2} \right) B''(r) + \\ &\frac{(9z^2+16)}{4r^2} B'^2(r) + \frac{z(3z^2-6z+8)B(r)}{2r^3} B'(r) + \\ &\frac{(z^4-4z^3+12z^2+16)}{4r^4} B^2(r) - \frac{8k}{r^4} B(r) + \frac{4k^2}{r^4}. \end{aligned} \quad (13)$$

Inserting the functional form of $B(r)$ into Eqs. (12) and (13), we obtain

$$R = b_1 k r^{-2} + b_2 m r^{-3-\frac{z}{2}} + b_3 q^2 r^{4-\lambda\sqrt{2z}} + b_4 V_0 r^{\gamma\sqrt{2z}} + \frac{(z^2+8z+24)}{6+z} \Lambda \quad (14)$$

$$\begin{aligned} R_{\alpha\beta\gamma\delta} R^{\alpha\beta\gamma\delta} &= \alpha_1 k^2 r^{-4} + \alpha_2 k m r^{-\frac{z}{2}-5} + \alpha_3 m^2 r^{-z-6} + \alpha_4 V_0^2 r^{2\gamma\sqrt{2z}} + \\ &\alpha_5 k V_0 r^{\gamma\sqrt{2z}-2} + \alpha_6 m V_0 r^{2\gamma\sqrt{2z}-\frac{z}{2}-3} + \alpha_7 q^4 r^{-2\lambda\sqrt{2z}-8} + \\ &\alpha_8 k q^2 r^{-\lambda\sqrt{2z}-6} + \alpha_9 m q^2 r^{-\frac{z}{2}-\lambda\sqrt{2z}-7} + \alpha_{10} V_0 q^2 r^{(\gamma-\lambda)\sqrt{2z}-4} + \\ &\alpha_{11} \Lambda k r^{-2} + \alpha_{12} \Lambda m r^{-\frac{z}{2}-3} + \alpha_{13} \Lambda V_0 r^{\gamma\sqrt{2z}} + \alpha_{14} \Lambda q^2 r^{-\lambda\sqrt{2z}-4} \\ &+ \frac{\Lambda^2}{(6+z)^2} [(z^2+4z+16)(z+4)z+96], \end{aligned} \quad (15)$$

where b_i 's and α_i 's are some constants related to z , γ and λ . The last (constant) term of this equation indicates that, in general, the asymptotic behavior of the solutions is AdS with an effective cosmological constant. However, considering the coefficient " $\frac{r}{r_0}$ " in the metric, one finds that the solutions are asymptotically Lifshitz-like solutions. We also find that the the curvature invariants are finite everywhere except for $r = 0$. In other words, there is a curvature singularity located at $r = 0$, which is simply a sign that the spacetime may contain a singular black hole, a singularity covered by an event horizon. Taking into account Eq. (11) and Fig. 1, it is clear that the singularity can be covered with an event horizon, and therefore, one can interpret it as a black hole. To speak more clearly, depending on the values of free parameters, the metric function may have two roots (black hole with an inner Cauchy horizon and an outer event horizon), an extreme root (extremal black hole) or no root (naked singularity: no black

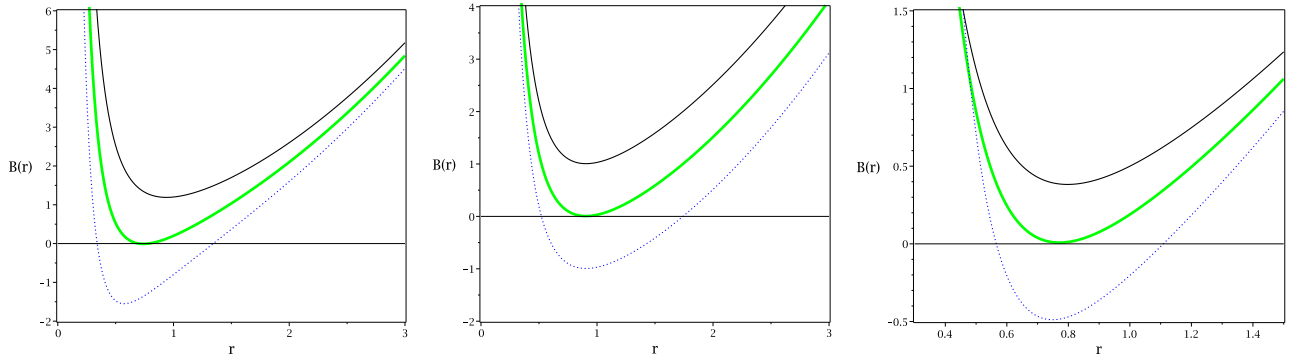


FIG. 1: $B(r)$ versus r for $\lambda = 1$, $\gamma = 1$, $q = 1$, $\Lambda = -1$, $V_0 = 1$, $r_0 = 1$.

Left panel: $z = 0$, $k = 1$, $m = 1.3$ (solid line), $m = 2.3$ (bold line) and $m = 3.3$ (dotted line).

Middle panel: $z = 0$, $m = 1.47$, $k = 1$ (solid line), $k = 0$ (bold line) and $k = -1$ (dotted line).

Right panel: $m = 2$, $k = 1$, $z = 0$ (solid line), $z = 0.07$ (bold line) and $z = 0.5$ (dotted line).

hole). In addition, according to the Fig. 1, we observe that $\lim_{r \rightarrow 0^+} B(r) = +\infty$, and therefore, the singularity is timelike and avoidable. It is also notable that for $z = 0$, Eq. (11) reduces to the Reissner-Nordström-AdS black hole solutions.

Regarding the mentioned geometrical properties of the solutions, we are in a position to examine the first law of thermodynamics. To do so, we should calculate the conserved and thermodynamic quantities.

First, we focus on the Hawking temperature. In order to calculate it, we can use the analytical continuation of the metric or the surface gravity interpretation. Both methods lead to the following unique result

$$T = \frac{B'(r_+)}{4\pi} \left(\frac{r_+}{r_0} \right)^{\frac{z}{2}} = \frac{\left(\frac{r_+}{r_0} \right)^{\frac{z}{2}} r_+}{4\pi} \times \left(\frac{k}{r_+^2} - \Lambda - \frac{q^2 \left(\frac{r_0}{r_+} \right)^{\lambda\sqrt{2z}}}{r_+^4} + \frac{V_0 \left(\frac{r_+}{r_0} \right)^{\gamma\sqrt{2z}}}{2} \right), \quad (16)$$

where we used the fact that r_+ is the largest real positive root of metric function, and therefore, $B(r_+) = 0$.

Another related quantity is the entropy. Since we are working with a Lifshitz-like model, applying the area law is challenging. Respecting the first law of thermodynamics, we can obtain the entropy by using $\delta S = \delta M/T$, and therefore, we need to have the finite mass.

Definition of finite mass for asymptotically AdS spacetimes has been given by Ashtekar-Magnon-Das (AMD) [36, 37]. They used the Penrose conformal completion techniques to map the boundary at infinity to a finite distance. The conserved quantities (such as mass and angular momentum in stationary spacetime) in the AMD approach are given in terms of the electric part of the Weyl tensor (see [38] for more details). The electric part of the Weyl tensor is corresponding to the Weyl tensor projected to the boundary, and one can find the finite conserved charge for the asymptotically AdS space for a given boundary conditions. Therefore, it is important to find the asymptotic (fall-off) behavior of the Weyl tensor in determining the conserved charges. It is worth mentioning that the Weyl tensor vanishes identically for the global AdS space, and therefore, the corresponding finite conserved charge vanishes as well in such a space. As a result, finite conserved charge in the AMD approach does not include the vacuum energy of the AdS space. Using the AMD approach, the total mass (per unit volume of $t = cte$ and $r = cte$ boundary: V_k) can be written as [36–39]

$$M = \frac{m_0}{8\pi} = \frac{m}{8\pi} r_0^{-\frac{z}{2}}, \quad (17)$$

where m is related to the geometrical mass ($m = m_0 r_0^{z/2}$) of the metric function which is calculated via $B(r_+) = 0$ as

$$m = \left[\frac{2k}{z+2} + \frac{V_0 r_+^2}{\Gamma} \left(\frac{r_+}{r_0} \right)^{\gamma\sqrt{2z}} + \frac{2q^2}{\Xi r_+^2} \left(\frac{r_0}{r_+} \right)^{\lambda\sqrt{2z}} - \frac{2\Lambda r_+^2}{6+z} \right] r_+^{(1-\frac{z}{2})}. \quad (18)$$

Considering Eq. (16), (17) and (18) with the validity of the first law ($\delta S = \delta M/T$), one can obtain the following relation for entropy (per unit volume V_k)

$$S = \frac{r_+^2}{4}, \quad (19)$$

which is the area law of black hole entropy. Considering the relation between the Faraday tensor and gauge potential, $F_{\mu\nu} = \partial_\mu A_\nu - \partial_\nu A_\mu$ with Eq. (10), we can find the nonzero component of the gauge potential is $A_t = -\int F_{tr} dr$, and therefore, the scalar potential U at the event horizon with respect to the reference ($r \rightarrow \infty$) can be written as

$$U = -\int_{r_+}^{\infty} F_{tr} dr = \frac{2q}{\Xi r_+} \left(\frac{r_0}{r_+}\right)^{\lambda\sqrt{2z}-\frac{z}{2}}. \quad (20)$$

In addition, in order to calculate the electric charge, we have to consider the projections of the electromagnetic field tensor on special hypersurfaces. The normal to such hypersurfaces is

$$u^0 = \frac{1}{N}, \quad u^r = 0, \quad u^i = -\frac{V^i}{N},$$

where N and V^i are the lapse function and shift vector. Using the Gauss law and the fact that the electric field is $E^\mu = g^{\mu\rho} e^{\lambda\phi} F_{\rho\nu} u^\nu$, we can obtain the electric charge Q (per unit volume V_k) by calculating the flux of the electric field at infinity, yielding

$$Q = \frac{q}{4\pi}. \quad (21)$$

Now, it is straightforward to confirm the first law of thermodynamics as

$$dM = TdS + UdQ, \quad (22)$$

since $T = \left(\frac{\partial M}{\partial S}\right)_Q$ and $U = \left(\frac{\partial M}{\partial Q}\right)_S$ are, respectively in agreement with those of calculated in Eqs. (16) and (20). As an important comment, we should note that although the first law of thermodynamics is satisfied, the corresponding Smarr relation is not valid. Such an anomaly is one of the motivations of working in the extended phase space thermodynamics which will be addressed in the next section.

III. EXTENDED PHASE SPACE, PHASE TRANSITION AND THERMAL STABILITY

A. van der Waals like behavior

Here, we want to work in the extended phase space thermodynamics. Considering the variation of the cosmological constant (motivated by the vacuum expectation value of a quantum field), we can study thermal stability in the extended phase space and look for a possible phase transition. In the context of extended phase space, we can regard the cosmological constant as a dynamical pressure $P = -\frac{\Lambda}{8\pi}$ [40–45]. Here, in order to define a suitable dynamical pressure, we should compare the r^2 -terms of Eq. (11), $\frac{-2\Lambda r^2}{6+z}$, with that of RN-AdS solutions, $\frac{-\Lambda r^2}{3}$. In other words, we can rewrite the r^2 -terms of Eq. (11) as $\frac{-2\Lambda r^2}{6+z} = \frac{-\Lambda_{\text{eff}} r^2}{3}$, and therefore,

$$P = -\frac{\Lambda_{\text{eff}}}{8\pi} = \frac{-3\Lambda}{4\pi(6+z)}, \quad (23)$$

with the thermodynamic volume as its conjugate quantity in the first law of thermodynamics. Regarding the cosmological constant as a thermodynamic pressure, we can find the extended version of the first law of thermodynamics with an additional volume-pressure term in the enthalpy representation

$$dM = TdS + UdQ + VdP, \quad (24)$$

where the mass of black hole is interpreted as the enthalpy ($M \equiv H$), i.e.,

$$M = H = \frac{m}{8\pi} r_0^{-\frac{z}{2}} = \frac{r_+}{8\pi} \left[\frac{2k}{z+2} + \frac{V_0 r_+^2}{\Gamma} \left(\frac{r_+}{r_0}\right)^{\gamma\sqrt{2z}} + \frac{2q^2}{\Xi r_+^2} \left(\frac{r_0}{r_+}\right)^{\lambda\sqrt{2z}} + \frac{8\pi P}{3} r_+^2 \right] \left(\frac{r_+}{r_0}\right)^{\frac{z}{2}}, \quad (25)$$

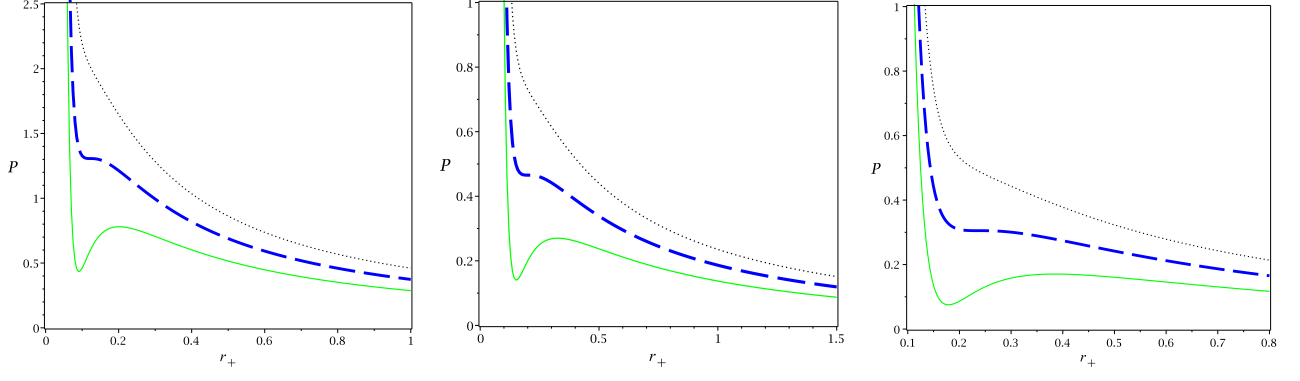


FIG. 2: P versus r_+ for $k = 1$, $\lambda = 1$, $\gamma = 1$, $q = 0.05$, $V_0 = 1$, $r_0 = 1$, and $T < T_c$ (solid line), $T = T_c$ (dashed line) and $T > T_c$ (dotted line). **Left panel:** $z = 0$, **Middle panel:** $z = 0.1$, **Right panel:** $z = 0.2$

where we used Eqs. (18) and (23). Using Eq. (24), the thermodynamic volume can be obtained as

$$V = \left(\frac{\partial M}{\partial P} \right)_{Q,S} = \frac{r_+^3}{3} \left(\frac{r_+}{r_0} \right)^{\frac{z}{2}}, \quad (26)$$

which is in agreement with $\int A dr = \int 4S dr = \frac{r_+^3}{3}$ for vanishing z .

After some calculations, we find that the conserved and thermodynamic quantities satisfy the following Smarr relation

$$\left(\frac{z}{2} + 1 \right) M = 2TS + \alpha UQ - 2PV - \beta V_0 \Delta_0, \quad (27)$$

where

$$\alpha = 1 + \frac{\lambda\sqrt{2z}}{2},$$

$$\beta = 2 + \gamma\sqrt{2z},$$

and Δ_0 is a conjugate quantity of V_0 which is defined as

$$\Delta_0 = \left(\frac{\partial M}{\partial V_0} \right)_{Q,S,P} = \frac{r_+^3}{8\pi\Gamma} \left(\frac{r_+}{r_0} \right)^{\gamma\sqrt{2z}+z/2}.$$

It is worth mentioning that for vanishing z , Eq. (27) reduces to the known Smarr relation $M = 2TS + UQ - 2P_{new}V$ ($P_{new} = P + \frac{V_0}{16\pi}$), as we expected.

Considering Eqs. (16) and (23), one can find the following equation of state

$$P = \frac{3}{4\pi r_+(6+z)} \left[\frac{4\pi T}{\left(\frac{r_+}{r_0} \right)^{\frac{z}{2}}} - \frac{k}{r_+} + \frac{\left(\frac{r_0}{r_+} \right)^{\lambda\sqrt{2z}} q^2}{r_+^3} - \frac{V_0 r_+}{2} \left(\frac{r_+}{r_0} \right)^{\gamma\sqrt{2z}} \right], \quad (28)$$

where r_+ is a function of thermodynamic volume as indicated in Eq. (26).

To investigate the existence of van der Waals like phase transition and critical behavior of the black hole, one can use the unique property of critical isothermal diagram in the $P - r_+$ plot, the inflection point,

$$\left(\frac{\partial P}{\partial r_+} \right)_T = \left(\frac{\partial^2 P}{\partial r_+^2} \right)_T = 0. \quad (29)$$

Traditionally, one should consider Eqs. (28) and (29) to obtain the three unknown critical quantities (r_c , T_c and P_c). Since we cannot obtain the analytical solutions of Eqs. (28) and (29), we continue with numerical analysis and give suitable tables and figures.

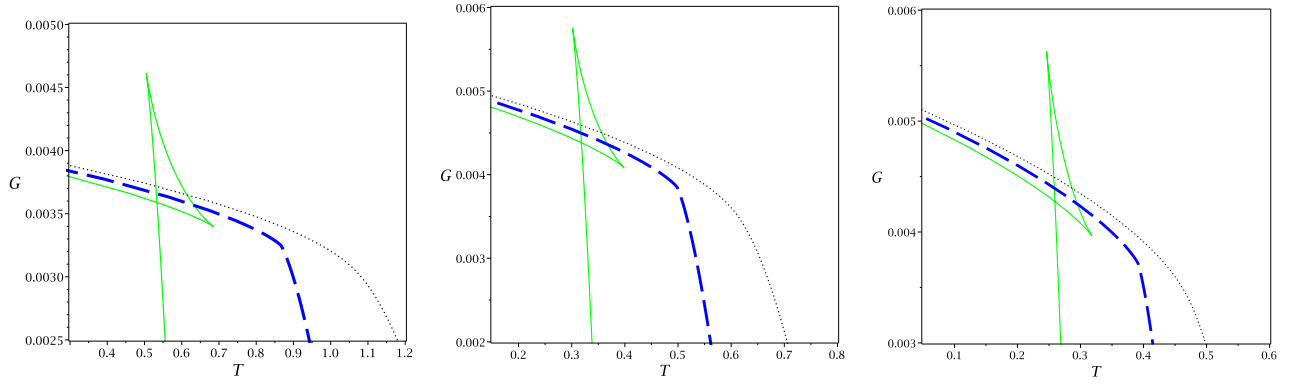


FIG. 3: Gibbs free energy versus temperature for $k = 1$, $\lambda = 1$, $\gamma = 1$, $q = 0.05$, $V_0 = 1$, $r_0 = 1$, and $P < P_c$ (solid line), $P = P_c$ (dashed line) and $P > P_c$ (dotted line). **Left panel:** $z = 0$, **Middle panel:** $z = 0.1$, **Right panel:** $z = 0.2$

In Fig. 2, we show the van der Waals like behavior of the system. In order to investigate the effects of various parameters on the critical behavior, one can study the following tables. According to these tables, we find that increasing the Lifshitz parameter (decreasing the electric charge) leads to increasing the critical temperature and pressure and decreasing the critical horizon. In addition, we find that in order to have critical behavior or van der Waals like phase transition, one has to imply some restrictions on the range of free parameters.

z	r_c	T_c	P_c
0.00	0.245	0.433	0.312
0.01	0.279	0.383	0.241
0.05	0.322	0.326	0.175
0.10	0.353	0.288	0.137
0.50	0.486	0.165	0.037
1.00	0.584	0.107	0.001
$z \geq 1.1$ anomaly anomaly negative			

q	r_c	T_c	P_c
0.001	0.008	10.42	286.64
0.005	0.031	2.99	20.64
0.01	0.054	1.74	6.64
0.05	0.201	0.498	0.465
0.10	0.353	0.288	0.137
0.20	0.613	0.162	0.027
$q \geq 0.3$ anomaly anomaly negative			

Left table: $k = 1$, $\lambda = 1$, $\gamma = 1$, $V_0 = 1$, $r_0 = 1$ and $q = 0.1$.

Right table: $k = 1$, $\lambda = 1$, $\gamma = 1$, $V_0 = 1$, $r_0 = 1$ and $z = 0.1$.

Another important quantity to investigate the possible phase transition (and also its order) is Gibbs free energy. In order to investigate the local thermodynamic stability one examine the positivity of the heat capacity while the equilibrium state of a system is corresponding to the global minimum of the Gibbs free energy. Since we shall study the thermodynamic behavior of the system in the canonical (fixed electric charge) ensemble, we can calculate the Gibbs free energy via $G = M - TS$ with the following explicit form

$$G = \frac{r_+}{16\pi} \left(\frac{r_+}{r_0} \right)^{\frac{z}{2}} \left[\frac{(2-z)k}{2+z} + \frac{(4-\Gamma)V_0 r_+^2}{2\Gamma \left(\frac{r_0}{r_+} \right)^{\gamma\sqrt{2z}}} + \frac{q^2(\Xi+4)}{\Xi r_+^2 \left(\frac{r_+}{r_0} \right)^{\lambda\sqrt{2z}}} - \frac{4\pi(z+2)P}{3r_+^{-2}} \right]. \quad (30)$$

The behaviour of Gibbs free energy is essential for finding possible thermodynamic phase transition and its order. However, it is often impossible to write, explicitly, the Gibbs free energy as a function of T , P and Q as $G = G(T, P, Q)$, and therefore, we have to use the implicit numerical calculation to plot $G - T$ diagram.

The behavior of Gibbs free energy with respect to temperature may be investigated via plotting the graph of isobaric $G - T$. Regarding Fig. 3, one finds the characteristics swallow-tail behavior of $G - T$ diagrams guarantees the existence of a first order phase transition.

As a final comment of this section, we should note that by adjusting the free parameters of the system, we can find a van der Waals like behavior for planar and hyperbolic topologies. For example, we can set $z = 2$, $\gamma = 2\lambda = 2r_0 = -1$ and $V_0 = 24$ for $k = -1$ (and $V_0 = 16$ for $k = 0$) to obtain

$$B(r) = 1 - \frac{m}{r^2} + \frac{2q^2}{r} - \frac{\Lambda r^2}{4}, \quad (31)$$

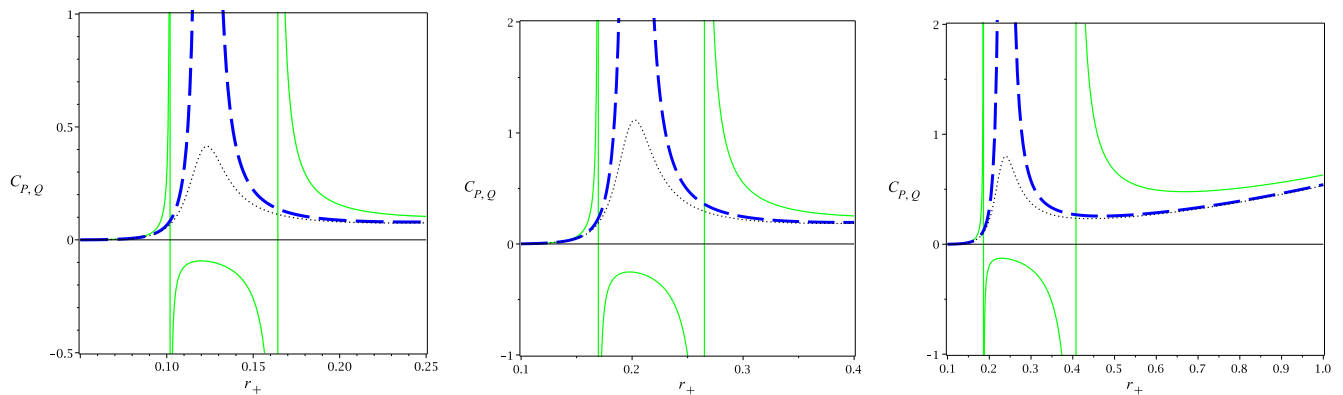


FIG. 4: Heat capacity versus r_+ for $k = 1$, $\lambda = 1$, $\gamma = 1$, $q = 0.05$, $V_0 = 1$, $r_0 = 1$, and $P < P_c$ (solid line), $P = P_c$ (bold line) and $P > P_c$ (dotted line). **Left panel:** $z = 0$, **Middle panel:** $z = 0.1$, **Right panel:** $z = 0.2$

which is nothing but a Reissner-Nordström-AdS black hole in which charge " q^2 " and mass " m " change their roles, and therefore, the possibility of a van der Waals like phase transition is evident.

B. Heat Capacity and Thermal Stability

Here, we will explain the criteria of having thermal stability of black holes. Analyzing the local thermal stability of a black hole can be performed in the canonical ensemble. In the context of extended phase space thermodynamics, the pressure and electric charge are kept constant in the canonical ensemble, and therefore, the stability criterion will be the positivity of heat capacity, i.e.,

$$C_{P,Q} = T \left(\frac{\partial S}{\partial T} \right)_{P,Q} = \frac{M_S}{M_{SS}}, \quad (32)$$

where $M_S = \left(\frac{\partial M}{\partial S} \right)_{P,Q}$ and $M_{SS} = \left(\frac{\partial^2 M}{\partial S^2} \right)_{P,Q}$. After some calculations and simplification, one finds

$$C_{P,Q} = \frac{V_0 r_+^4 \left(\frac{r_+}{r_0} \right)^{\gamma\sqrt{2z}} - 2q^2 \left(\frac{r_0}{r_+} \right)^{\lambda\sqrt{2z}} + \frac{2r_+^2 [3k + 4\pi(z+6)Pr_+^2]}{3}}{V_0 r_+^2 (\Gamma - 4) \left(\frac{r_+}{r_0} \right)^{\gamma\sqrt{2z}} + \frac{2(\Xi+4)q^2}{r_+^2} \left(\frac{r_0}{r_+} \right)^{\lambda\sqrt{2z}} + \frac{2(z-2) [3k + \frac{4\pi(z+6)(z+2)}{(z-2)} Pr_+^2]}{3}}. \quad (33)$$

Regarding the heat capacity, it is notable that its divergence points may be interpreted as phase transitions of our system. In order to have a van der Waals like behavior, we should obtain two divergence points for the heat capacity with $C_{P,Q} < 0$ between them. Figure 4 is plotted to confirm the existence of a first order phase transition. We find that for $P < P_c$, there are two divergence points related to a first order phase transition. For $P \rightarrow P_c$, the two divergence points emerge to one and negative region disappears at $P = P_c$ which is related to the critical point. As expected, for $P > P_c$, there is no divergency for the heat capacity and black holes are thermally stable.

C. Response functions

One of the interesting methods including the fundamental thermodynamic information is extracting the response functions of the system under consideration. One of these response functions is the heat capacity which is related to the second derivatives of the Gibbs free energy with respect to the temperature, as $C_{P,Q} = T \left(\frac{\partial S}{\partial T} \right)_{P,Q} = \frac{T}{\left(\frac{\partial^2 M}{\partial S^2} \right)_{P,Q}} = -T \left(\frac{\partial^2 G}{\partial T^2} \right)_{P,Q}$. Other (Gibbsian) response functions are related to the second derivatives of the Gibbs free energy with respect to the independent thermodynamic quantities. Regarding the functional form of the Gibbs free energy $G = G(T, Q, P)$ given in Eq. (30), one finds that the response functions can be related to $\left(\frac{\partial^2 G}{\partial P^2} \right)_{T,Q}$, $\left(\frac{\partial^2 G}{\partial Q^2} \right)_{T,P}$,

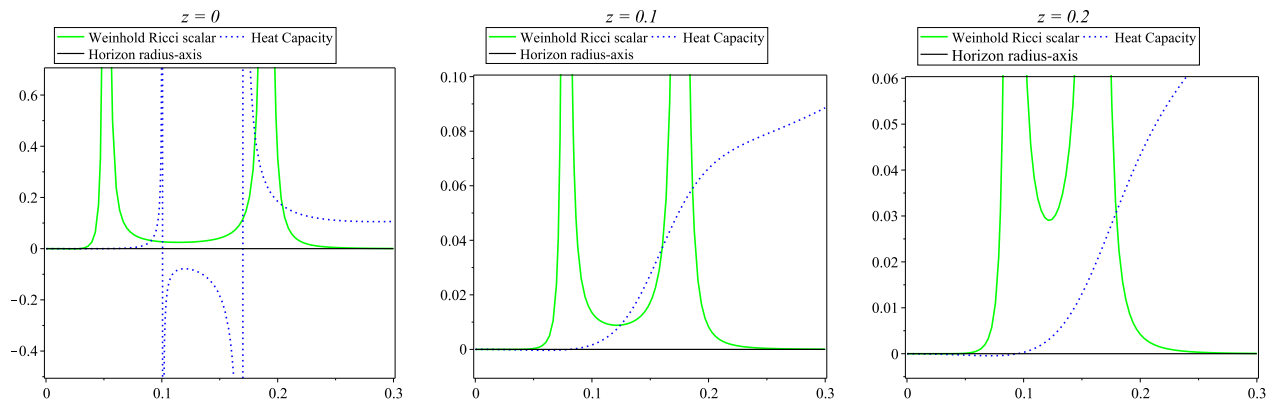


FIG. 5: Heat Capacity (dotted line) and the Ricci scalar of Weinhold metric (solid line) versus r_+ for $k = 1$, $\lambda = 1$, $\gamma = 1$, $q = 0.05$, $V_0 = 1$, $r_0 = 1$ and $P < P_c$. **Left panel:** $z = 0$, **Middle panel:** $z = 0.1$, **Right panel:** $z = 0.2$ (*For more clarifications we used different scales*).

$\left(\frac{\partial^2 G}{\partial T \partial P}\right)_Q$, $\left(\frac{\partial^2 G}{\partial T \partial Q}\right)_P$ and $\left(\frac{\partial^2 G}{\partial P \partial Q}\right)_T$. Since we look for the possible van der Waals like phase transition, in this paper, we focused on the heat capacity and put other response functions aside. However, one can investigate divergence points of other response functions and their relation to novel phase transitions.

D. Geometrical thermodynamics

Regarding the geometrical thermodynamic method, the thermodynamic phase space and the space of equilibrium state are involved. Many attempts were made to describe the thermodynamic behavior of black holes, geometrically, based on the defined metric on the equilibrium space [20, 21]. In particular, the Weinhold and Ruppeiner metrics were used in order to link the curvature singularities of defined thermodynamic metric and heat capacity divergences, directly, but the results caused contradictory outcomes. There are many examples that the singularities of these metrics are not located on the phase transition points, or in some cases, there are a number of singularities before and after those points. As an example, for the Kerr black hole the Weinhold metric predicts that there is no phase transition, while Ruppeiner one predicts that with a certain thermodynamic potential, the phase transition is in accordance with the standard results of thermal properties of black holes [24, 25].

It is shown that these inconsistencies arise from the fact that both Weinhold and Ruppeiner metrics are not Legendre invariant, which makes the metrics not suitable to describe the thermodynamics of the system. Legendre invariance plays a crucial role in geometrical thermodynamics and it means when a particular demonstration is chosen for description of a system, the Legendre transformations in the new form should have the same information as the initial representation. Therefore, Legendre invariance is one of the important characteristics of thermodynamic metrics when making the desired geometry.

In order to resolve such problems, Quevedo and his colleagues proposed a method to find the metric that is Legendre invariant [24, 25]. Although the Quevedo metric solved most of the problems of the previous metrics, it faced a problem in several specific cases. To solve its problem, a new metric has been recently introduced [26] in which the problem of additional singularities that are not consistent with any of the phase transition points is not observed.

In what follows, we intend to introduce these thermodynamical metrics and discuss their results in our case. The first metric which was introduced by Weinhold is given by

$$dS_W^2 = M g_{ab}^W dX^a dX^b, \quad (34)$$

where M is the mass which is a function of extensive quantities such as entropy and electric charge and hereafter we use the notation $M_X = \partial M / \partial X$ and $M_{XX} = \partial^2 M / \partial X^2$. Finding divergence points of the Ricci scalar is interesting for us. In order to find these points, we involve the denominator of the Ricci scalar, since its numerator is a finite smooth function. The denominator of Weinhold Ricci scalar for our system is

$$\text{denom}(R_W) = M^3 (M_{SS} M_{QQ} - M_{SQ}^2)^2. \quad (35)$$

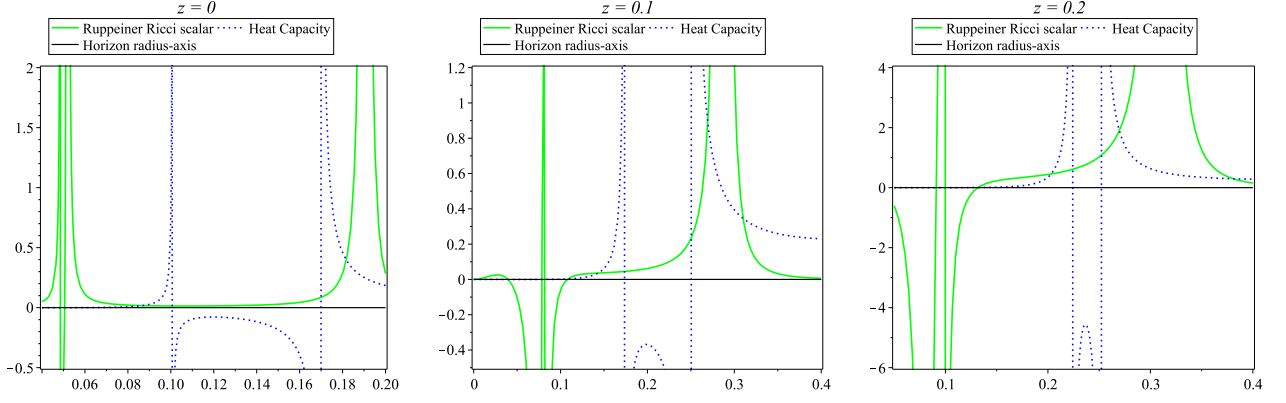


FIG. 6: Heat Capacity (dotted line) and the Ricci scalar of Ruppeiner metric (solid line) versus r_+ for $k = 1$, $\lambda = 1$, $\gamma = 1$, $q = 0.05$, $V_0 = 1$, $r_0 = 1$ and $P < P_c$. **Left panel:** $z = 0$, **Middle panel:** $z = 0.1$, **Right panel:** $z = 0.2$ (*For more clarifications we used different scales*).

It is clear that there is at least a divergence point for the Ricci scalar when $M_{SS}M_{QQ} = M_{SQ}^2$, which is not consistent with any divergency of the heat capacity. We plot both the Ricci scalar and heat capacity in Fig. 5 to inquire into the mentioned behavior. As one can see, divergence points of the heat capacity are not coincidence with those of the Ricci scalar of Weinhold metric.

The Ruppeiner metric was the second metric which is related to Weinhold metric by a Legendre transformation as

$$dS_R^2 = -MT^{-1}g_{ab}^W dX^a dX^b. \quad (36)$$

Taking into account the relation between these two metrics, one can find the denominator of Ruppeiner's Ricci scalar as

$$\text{denom}(R_R) = M^3 T (M_{SS}M_{QQ} - M_{SQ}^2)^2. \quad (37)$$

It is evident that the same additional divergency of the Weinhold metric is presented here. In Fig. 6, we plot the Ruppeiner Ricci scalar which shows that its divergencies are not matched with those of the heat capacity, like Weinhold case.

As these two metrics cannot properly describe our system, we employ Quevedo metric in order to remove such failures. The Quevedo metric has the following form

$$dS_Q^2 = \Omega (-M_{SS}dS^2 + M_{QQ}dQ^2), \quad (38)$$

where $\Omega = SM_S + QM_Q$. The denominator of Quevedo Ricci scalar is

$$\text{denom}(R_Q) = M_{SS}^2 M_{QQ}^2 (SM_S + QM_Q)^3. \quad (39)$$

Although vanishing of M_{SS} indicates that such divergency is the same as that of the heat capacity, $M_{QQ} = 0$ and $SM_S + QM_Q = 0$ deal with additional (inconsistent) divergencies. We can find the mentioned behavior in Fig. 7. It is evident that although for some arbitrary values of free parameters, Quevedo's approach leads to consistent result (see Fig. 7), one may adjust free parameters to find at least one extra divergency. It is clear that such an extra divergency comes from the possible real root of the following relation which is observed in denominator of Quevedo's Ricci scalar

$$S \frac{dM(S, Q)}{dS} + Q \frac{dM(S, Q)}{dQ} = 0. \quad (40)$$

In addition, regarding the up panels of Fig. 7, we find that there is no consistency for the root of $C_{Q,P}$. So, one can regard another consistent thermodynamical metric.

Finally, we employ the HPEM metric which has a different structure from other metrics as the following form

$$ds_{HPEM} = \frac{SM_S}{M_{QQ}^3} (-M_{SS}dS^2 + M_{QQ}dQ^2). \quad (41)$$

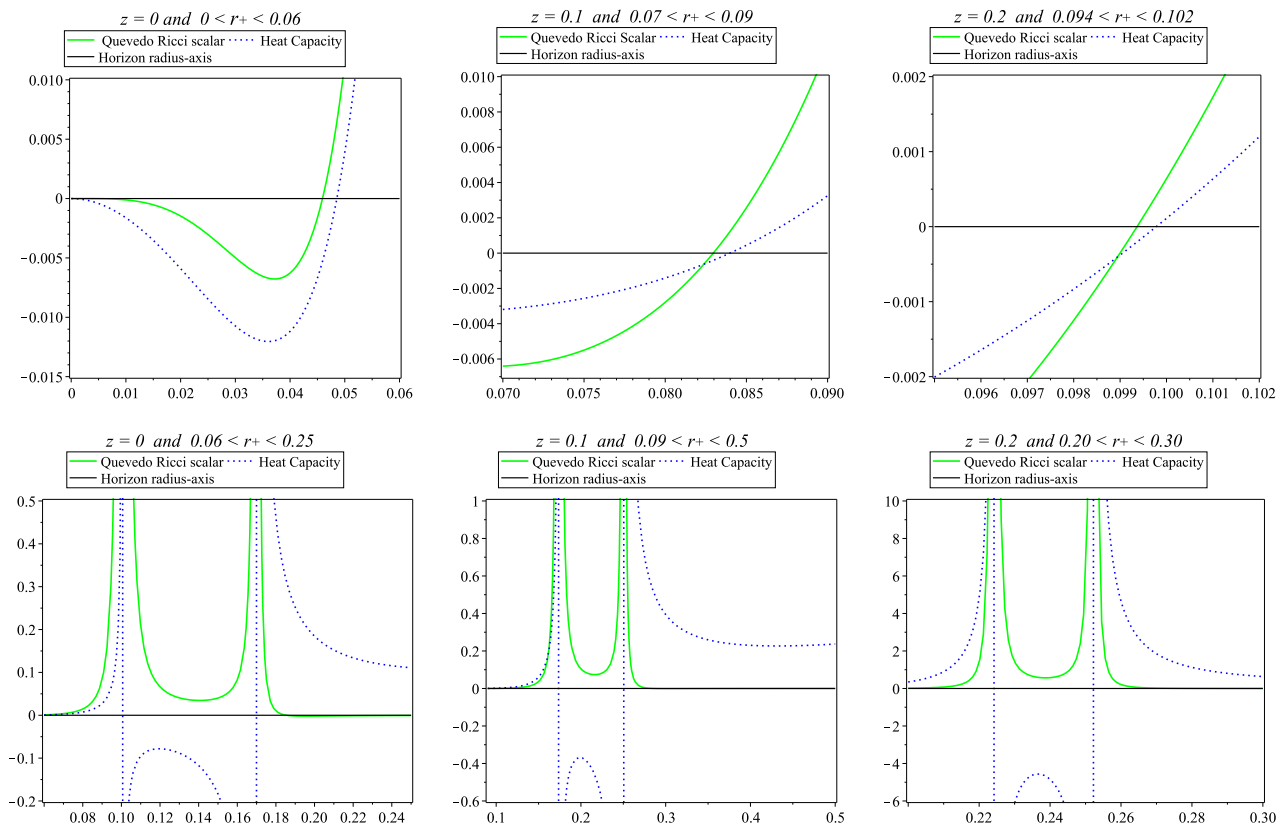


FIG. 7: Heat Capacity (dotted line) and the Ricci scalar of Quevedo metric (solid line) versus r_+ for $k = 1$, $\lambda = 1$, $\gamma = 1$, $q = 0.05$, $V_0 = 1$, $r_0 = 1$ and $P < P_c$. **Left panels:** $z = 0$, **Middle panels:** $z = 0.1$, **Right panels:** $z = 0.2$ (For more clarifications we used different scales).

It can be seen that the HPEM metric is the same as Quevedo's one up to a conformal factor, and this fact guarantees the Legendre invariancy of HPEM metric. Calculations show that the denominator of the Ricci scalar of this metric is simplified as

$$\text{denom}(R_{HPEM}) = 2S^3 M_{SS}^2 M_S^3. \quad (42)$$

According to Eq. (42), one finds two sets of divergencies. One of them ($M_S = 0$) related to the root of temperature and the other ($M_{SS} = 0$) corresponds to divergence points of the heat capacity. For more clarifications, we plot Fig. 8. In this figure, one finds different behaviors of the HPEM Ricci scalar before and after the divergence points and root (zero T) of the heat capacity. In other words, the divergence points of the Ricci scalar related to the root of heat capacity could be distinguished from the divergencies related to phase transition points based on the curvature scalar behavior.

IV. CONCLUSION

The scalar-tensor theory of gravity is one of the well-known alternative theories of Einstein gravity which is motivated by the low-energy limit of superstring theory. This theory can be represented in the two conformally related (equivalent) frames, the Jordan frame in which the scalar field is non-minimally coupled to the metric tensor and the Einstein frame in which the scalar field is minimally coupled to the metric tensor.

In this paper, we considered one of the special models of this theory in the Einstein frame and investigated its Lifshitz like black hole solutions with different horizon topologies. We found that these solutions have an asymptotically Lifshitz like behavior.

Then, we studied thermodynamic properties of the solutions in the extended phase space and found that these black holes may behave like a van der Waals system depending on the choice of the Lifshitz parameter. In other words,

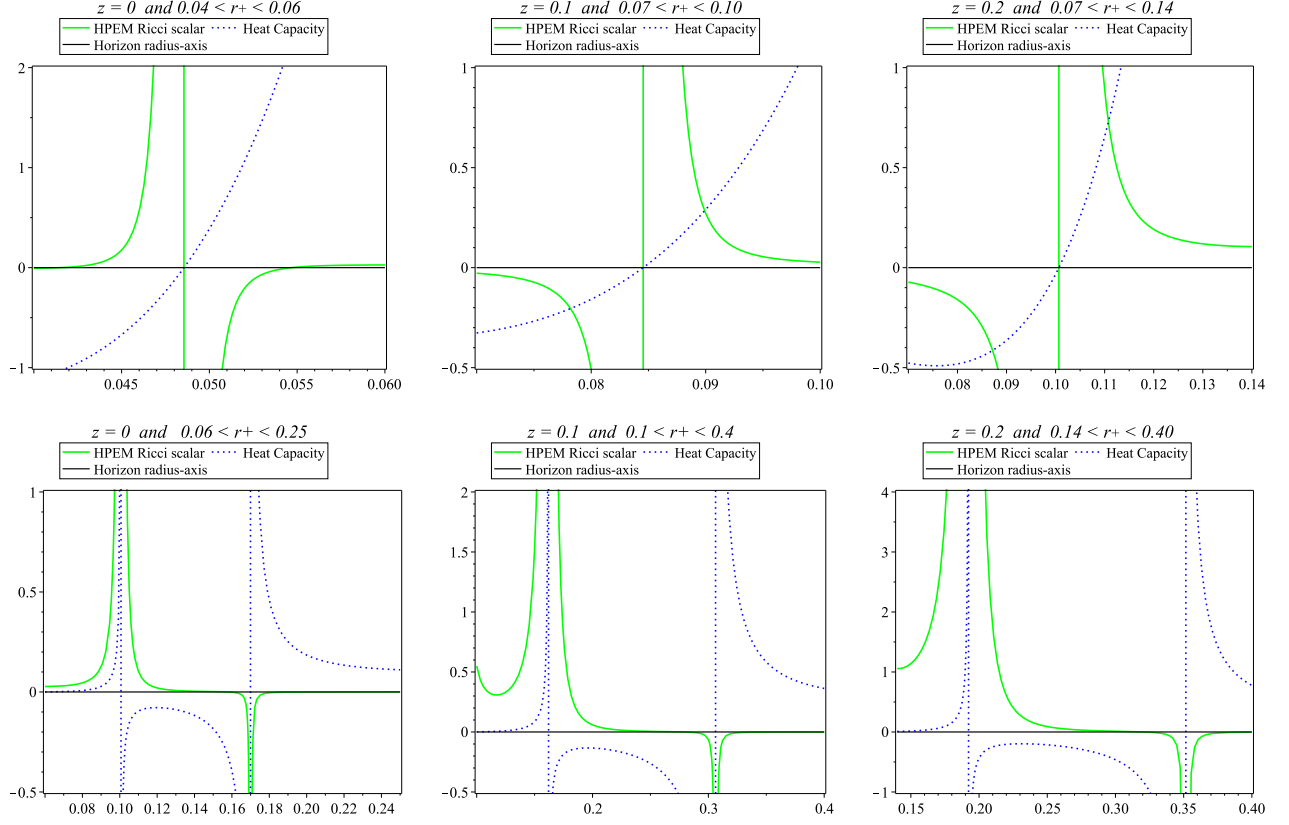


FIG. 8: Heat Capacity (dotted line) and the Ricci scalar of HPEM metric (solid line) versus r_+ for $k = 1$, $\lambda = 1$, $\gamma = 1$, $q = 0.05$, $V_0 = 1$, $r_0 = 1$ and $P < P_c$. **Left panels:** $z = 0$, **Middle panels:** $z = 0.1$, **Right panels:** $z = 0.2$ (For more clarifications we used different scales).

one can find a first order phase transition for $T < T_c$ in isotherm $P - V$ diagram (or correspondingly for $P < P_c$ in $G - T$ plots). We also numerically calculated the critical quantities and showed that these critical quantities depend on the Lifshitz parameter. Interestingly, we found a van der Waals like phase transition for topological black holes with planar and hyperbolic event horizons.

In order to investigate thermal stability, we calculated the heat capacity and found that the results are completely in agreement with our previous conclusions in the extended phase space. For the sake of completeness, we investigated the phase transition and critical points by use of different models of geometrical thermodynamics and interpreted their results.

It is interesting to investigate the conformally related black hole solutions in the Jordan frame and compare their thermodynamic properties with our results. We should note that although both Einstein and Jordan frames are equivalent, the conformally related black hole solutions may have different properties. In addition, one can apply metric perturbations to investigate dynamical stability of the solutions. Moreover, one may follow the work of Ref. [46] and investigate new aspect of thermodynamic properties of these black holes by regarding the Hawking radiation to define an alternative Smarr relation with new pressure, volume and entropy. We leave these subjects for the future work.

Acknowledgements

We would like to thank the anonymous referees for their valuable comments which improved the quality of this manuscript significantly. We wish to thank Shiraz University Research Council. SHH would like to thank the hospitality of the Institute of Theoretical Physics, Faculty of Mathematics and Physics, Charles University during his

short visit.

-
- [1] B. P. Abbott et al., Phys. Rev. Lett. **116** (2016) 061102.
 - [2] P. Horava, Phys. Rev. D **79** (2009) 084008.
 - [3] P. Horava, Phys. Rev. Lett. **102** (2009) 161301.
 - [4] M. Visser, Phys. Rev. D **80** (2009) 025011.
 - [5] M. Visser, [arXiv:0912.4757].
 - [6] D. Anselmi and M. Halat, Phys. Rev. D **76** (2007) 125011.
 - [7] T. Fujimori, T. Inami, K. Izumi and T. Kitamura, Phys. Rev. D **91** (2015) 125007.
 - [8] T. Fujimori, T. Inami, K. Izumi and T. Kitamura, Prog. Theor. Exp. Phys. **2016** (2016) 013B08.
 - [9] J. D. Bekenstein, Phys. Rev. D **7** (1973) 2333.
 - [10] S. W. Hawking, Commun. Math. Phys. **43** (1975) 199.
 - [11] S. W. Hawking and D. N. Page, Commun. Math. Phys. **87** (1983) 577.
 - [12] J. M. Bardeen, B. Carter, S. W. Hawking, Commun. Math. Phys. **31** (1973) 161.
 - [13] S. W. Hawking, Nature **248** (1974) 30.
 - [14] S. W. Hawking, Commun. Math. Phys. **43** (1975) 199.
 - [15] A. Strominger and C. Vafa, Phys. Lett. B **379** (1996) 99.
 - [16] C. Rovelli, Phys. Rev. Lett. **77** (1996) 3288.
 - [17] A. Strominger, JHEP **9802** (1998) 009.
 - [18] J. Gibbs, *The collected works* Vol. 1, Thermodynamics (Yale University Press, 1948).
 - [19] C. Charathodory, *Untersuchungen uber die Grundlagen der thermodynamik*, Gesammelte Mathematische Werke, Band 2 (Munich, 1995).
 - [20] F. Weinhold, J. Chem. Phys. **63** (1975) 2479.
 - [21] F. Weinhold, J. Chem. Phys. **63** (1975) 2484.
 - [22] G. Ruppeiner, Phy. Rev. A **20** (1979) 1608.
 - [23] G. Ruppeiner, Rev. Mod. Phys. **67** (1995) 605.
 - [24] H. Quevedo and R. D. Zarate, Re. Mex. Fis. **49** (2003) 125.
 - [25] H. Quevedo, J. Math. Phys. **48** (2007) 013506.
 - [26] S. H. Hendi, S. Panahian, B. Eslam Panah and M. Momennia, Eur. Phys. J. C **75** (2015) 507.
 - [27] S. H. Hendi, S. Panahian and B. Eslam Panah, Adv. High Energy Phys. **2015** (2015) 743086.
 - [28] S. H. Hendi, A. Sheykhi, S. Panahian and B. Eslam Panah, Phy. Rev. D **92** (2015) 064028.
 - [29] S. Soroushfar and S. Upadhyay, Phys. Lett. B **804** (2020) 135360
 - [30] T. Vetsov, Eur. Phys. J. C **79** (2019) 71.
 - [31] M. Chabab, H. El Moumni, S. Iraoui and K. Masmar, Eur. Phys. J. C **79** (2019) 342.
 - [32] M. Alishahiha, E. O Colgain and H. Yavartanoo, JHEP **11** (2012) 137.
 - [33] D. Momeni, R. Myrzakulov and L. Sebastiani and M. R. Setare, Int. J. Geom. Meth. Mod. Phys. **12** (2015) 1550015.
 - [34] J. Tarrío and S. Vandoren, JHEP **09** (2011) 017.
 - [35] M. Taylor, [arXiv:0812.0530].
 - [36] A. Ashtekar and A. Magnon, Class. Quantum Gravit. **1** (1984) L39.
 - [37] A. Ashtekar and S. Das, Class. Quantum Gravit. **17** (2000) L17.
 - [38] D. P. Jatkar, G. Kofinas, O. Miskovic and R. Olea, Phys. Rev. D **89** (2014) 124010.
 - [39] R. Emparan, H. S. Reall, Living Rev. Relativ. **11** (2008) 6.
 - [40] D. Kubiznak and R. B. Mann, JHEP **07** (2012) 033.
 - [41] D. Kastor, S. Ray and J. Traschen, Class. Quantum Gravit. **26** (2009) 195011.
 - [42] B. P. Dolan, Class. Quantum Gravit. **28** (2011) 125020.
 - [43] B. P. Dolan, Class. Quantum Gravit. **28** (2011) 235017.
 - [44] B. P. Dolan, Phys. Rev. D **84** (2011) 127503.
 - [45] M. Cvetič, G. Gibbons, D. Kubiznak and C. Pope, Phys. Rev. D **84** (2011) 024037.
 - [46] T. S. Biro, V. G. Czinner, H. Iguchi and P. Van, Phys. Lett. B **803** (2020) 135344.